IEICE TRANS. FUNDAMENTALS, VOL.E102–A, NO.1 JANUARY 2019

INVITED PAPER *Special Section on Wideband Systems*

Practical Performance and Prospect of Underwater Optical Wireless Communication

—— Results of Optical Characteristic Measurement at Visible Light Band under Water and Communication Tests with the Prototype Modem in the Sea ——

Takao SAWA[†a)], ***Member***, **Naoki NISHIMURA**[††], **Koji TOJO**[††], ***and*** **Shin ITO**[†††], ***Nonmembers***

SUMMARY Underwater optical wireless communication has been merely a theory for a long time because light sources are too weak to use them as emitters for communications. In the past decade, however, underwater optical wireless communications have used laser diodes or light emitting diodes as emitters with visible light in high brightness with low power consumption. Recently, they have become practical. As described in this paper, recent trends of underwater optical wireless communication study, practical modems and prospective uses of underwater optical wireless communication are presented first. Next, optical characteristics of the seawater in various conditions are explained based on the experimental data measured using the profiler for underwater optics produced especially for this study. Then the prototype underwater optical wireless communication modem developed by our team is introduced. It was tested in several sea areas, which confirmed bi-directional communication in the 120 m range at 20 Mbps and a remote desktop connection between under water vehicles at 100 m range. In addition, one modem was set in air; other was set in water. The modems mutually communicated directly through the sea surface.

key words: *chlorophyll, LD, turbidity, UOWC, VLC*

GLOSSARY

AGC	Auto gain control
AM	Amplitude modulation
APD	Avalanche photodiode
AUV	Autonomous underwater vehicle
BCH	Bose–Chaudhuri–Hocquenghem
CRC	Cyclic redundancy check
DPIM	Digital pulse interval modulation
FTU	Formazin turbidity unit
IM/DD	Intensity modulation and direct detection
IrDA	Infrared data association
LD	Laser diode
LED	Light emitting diode
Li-Fi	Light fidelity
MEMS	Micro-electromechanical system
OFDM	Orthogonal frequency-division multiplexing
OOK	On–off keying
PD	Photo diode
PLL	Phase lock loop
PM	Pulse modulation
PMT	Photomultiplier tube
PPM	Pulse period modulation
PWM	Pulse width modulation
RS	Reed–Solomon
RTE	Radiative transfer equation
S/N	Signal-to-noise ratio
SI	Swarm intelligence
UOWC	Underwater optical wireless communication
V2V	Vehicle-to-vehicle

Manuscript received August 3, 2018.
Manuscript revised September 26, 2018.
[†]The author is with JAMSTEC, Yokosuka-shi, 237-0061 Japan.
[††]The authors are with Shimadzu, Kyoto-shi, 604-8511 Japan.
[†††]The author is with SAS, Tokyo, 110-0016 Japan.
a) E-mail: sawa@jamstec.go.jp
DOI: 10.1587/transfun.E102.A.156

1. Introduction

Radio waves attenuate quickly in seawater, which as an electrolyte. Therefore acoustic communication is usually used for underwater wireless communication. Attenuation of electromagnetic waves including visible light and acoustic waves in water has been studied well [1], [2]. Figure 1 is a simple graph of the respective attenuations of electromagnetic and acoustic waves. The attenuation of acoustic waves is extremely low. The wave speed is also low: around 1500 m/s. Furthermore, the frequency is low, of kilohertz to hundreds of kilohertz order. These facts mean that the speed of acoustic communications can not become as high as that of radio communications, theoretically.

For example, if we transfer a digital picture having data size of 1 Mbyte using acoustic communication, it will take

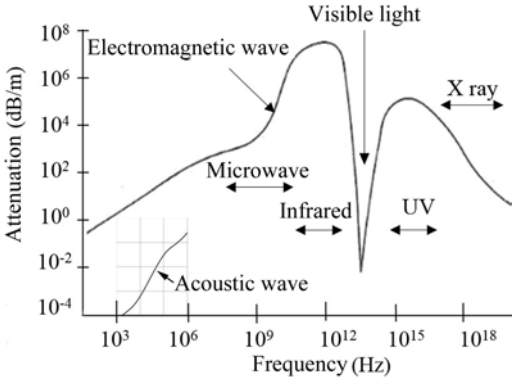

Fig. 1 Attenuations of electromagnetic wave including visible light and acoustic waves in water.

14 min. However, the visible light attenuation is not high. Its frequency is very high: around 800 THz.

Therefore, the study of underwater optical wireless communication (UOWC) was started from 1960s to communicate in the sea at higher speeds than acoustic communication, when lasers able to emit light at high optical densities were invented. The technique of laser ranging and scanning has been studied from that time; analysis of optical characteristics in the ocean also started at that time [3]. Optical attenuation for every wave frequency had already been measured in the 1970s [4].

Light of around 450 nm is absorbed only slightly in pure water. However, the wavelength of the lowest absorption in water becomes longer in proportion to increased absorption. Such increase results from increase of suspended particles like marine snow [5]. In addition, ships and underwater vehicles are usually unstable because of ocean waves and currents. That instability leads to error of axis alignment for collimated light such as lasers. It causes loss of wireless optical links. Expanding the width or laser beam diameter, makes the communication range too short for practical use.

In recent years, gallium nitride semiconductor light sources, such as laser diodes (LDs) and light emitting diode (LEDs), have progressed rapidly. High brightness but low power consumption of light sources has been achieved with these diodes. Lighting equipment is rapidly shifting from filament and fluorescent light to diodes now. The diodes have high energy efficiency and high response sufficient to achieve high communication speed over 1 MHz. Performance of UOWC has been improved greatly using LD and LED.

Many studies of UOWC were published in several years. Furthermore, some commercial UOWC modems were released. Our team started developing UOWC in 2015, first trying underwater communication in early 2016, and achieving communication with over 100 m range at 20 Mbps in bi-directional with prototype UOWC modem.

As described herein, recent trends and prospective uses of UOWC are presented to some degree in Sect. 2. Optical characteristics of the sea in various conditions are explained based on experimental data in Sect. 3. A prototype UOWC modem developed by our team and test results of the modem are explained in Sect. 4. Conclusions are presented in Sect. 5.

2. Recent Trends of UOWC

Some reviews have examined UOWC [6], [7]. Because these papers described the current status of UOWC well, recent trends of UOWC are expressed in this chapter referring to these papers.

2.1 Trend of UOWC Study

The study of UOWC emphasizes channel characterization, modulation, and coding techniques.

Light is attenuated quickly in water, so channel characterization strongly affects UOWC performance. Water absorbs and scatters the light. The amount of attenuation caused by these affections can be calculated theoretically using kinetic theory of molecular water [1]. However, seas in which major fields of whole underwater communication, have suspended particles such as marine-snow, chlorophyll, and very small detritus (or clay). Absorption of light by seawater is low: around 400–500 nm [6]. Still, absorption by marine-snow and detritus becomes high in inverse proportion to the light wavelength [7], [8]. Absorption by chlorophyll is high, occurring at around 450–660 nm [9]. The quantity of particles differs among seasons, areas, and water depths. Light attenuation is difficult to estimate without measuring the quantity.

If we attain attenuation, then the light power in the sea will be calculated simply from Beer–Lambert's law [10] and will be described as

$$I = I_0 e^{-c(\lambda)z}, \tag{1}$$

where I and I_0 respectively represent the power of received and transmitted light, z denotes the transmission distance, and $c(\lambda)$ is the attenuation coefficient at wavelength λ of the light.

For more precise results that incorporate scattering and dispersion, radiative transfer equation (RTE) is often employed [11]. Furthermore, the RTE is often solved numerically using Monte Carlo method [12]. Particles diffuse light. Misalignment usually occurs where waves and currents exist. These are calculated using the method. The methods can also estimate reflection by the water surface, so effects by multipath and UOWC over non-line-of-sight paths were studied using the methods [13]. Turbulence, which changes the refractive index of water in a short time, is important for UOWC performance. It was studied based on atmospheric optical turbulence channel models [14].

Frequency of light is very high: around 500 THz. It is difficult to use phase information in water, which causes high dispersion at that frequency. Coherent systems for optical wireless light communication will become complex and entail high costs [15] for these reasons. Furthermore, the phase lock loop (PLL) for synchronization between a transmitter and receiver is difficult to stabilize.

Therefore, intensity modulation and direct detection (IM/DD) are preferred and reasonable for UOWC. Modulation of UOWC in many studies is on–off keying (OOK). That keying is a kind of amplitude modulation (AM), which is simple and easy to put into the communication system. Pulse modulation (PM), such as pulse period modulation (PPM), pulse width modulation (PWM), and digital pulse interval modulation (DPIM), have been tried for UOWC.

Orthogonal frequency-domain multiplexing (OFDM) has also been tried. Some remarkable performance was achieved [16].

A main purpose of coding is to reduce communication errors, or to correct errors with redundant information in the coded data. Reed–Solomon (RS) code has been used from the early UOWC study [17]. Complex coding technique, such as LDPC and Turbo code, have been tried recently

[18]. The coding increases the signal-to-noise ratio (S/N). The code gain is generally from 2.5 to 9.5 dB [19]. Still, Bose–Chaudhuri–Hocquenghem (BCH) code and cyclic redundancy check (CRC) code are practical, especially at low S/N.

2.2 Experimental and Commercial UOWC Modems

Almost all UOWC use LDs or LEDs to emit light as a signal carrier. Comparison of LDs and LEDs reveals that LDs perform better for communication: the speed is high, the beam band is narrow, and the beam can be collimated accurately. However, LEDs are low-cost materials that can emit lightly consuming low-energy fluorescence. Therefore, high-speed and long-range UOWC often employ LDs, whereas LEDs are suitable for small UOWC modems in a short range.

Detectors for UOWC are selected from photodiodes (PDs), avalanche photodiodes (APD), and photomultiplier tubes (PMTs). Their sensitivity is higher in the order of PMTs, APDs, and PDs. However, the cost becomes higher in that order, also. The system becomes complex also in the same order. Detectors are usually chosen while accounting for the study purpose.

A research team at Woods Hole Ocean Institute tested their LED-based UOWC system for data retrieval from an ocean bottom station. 1 Mbps communication speed at 138 m range was accomplished through testing [20]. The team also tried LD-based UOWC, which achieved 5 Mbps speed at 200 m [21]. These outcomes were used for Bluecomm, a commercial UOWC produced by Sonardyne.

MIT researchers tried an LED-based UOWC modem called AquaOptical II. The system sent data at 2 Mbps speed at over 50 m range. It achieved real-time video delivery [22].

A 16-QAM-OFDM UOWC system that employed TO-9 packaged fiber-pigtailed LD was tried by another team. That team recorded 4.8 Gbps communication speed over 5.4 m distance in a water tank [23].

Unique wireless communication systems using retro-reflectors were tried in UOWC. One modem sends light to the other modem with a reflector, without a light source. The light reflected by the reflector is modulated. It comes to be signals from the modem. The research group of North Carolina State University assessed a system with a retro-reflector based on a micro-electromechanical system (MEMS) [24]. They achieved 1 Mbps communication at 5 m distance in a water tank.

In Japan, some practical UOWC modems have been released. Toyo Electric Corp., in cooperation with Taiyo Yuden Co., Ltd., developed a UOWC modem for HD video data transfer [25]. The modem can transfer data at 50 Mbps speed in at a 20 m range. Kawasaki Heavy Industries Ltd. produced an LED-based UOWC modem [26]. The modem has wide directivity and was loaded on an autonomous underwater vehicle (AUV) for data transfer between the AUV and an underwater station.

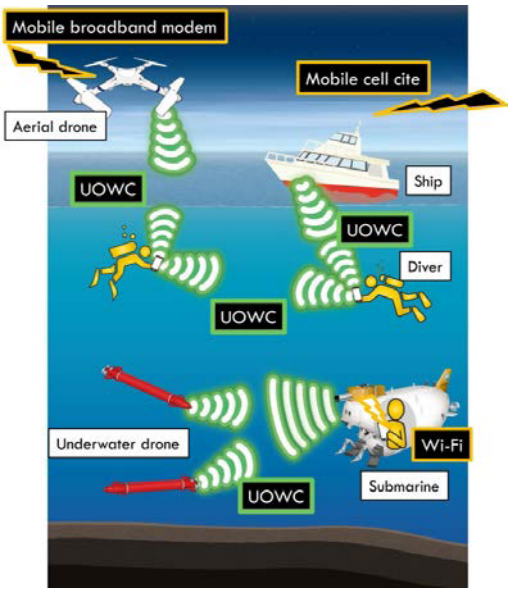

Fig. 2 Prospective usage of UOWC.

2.3 Prospect of UOWC and Its Usage

Our tests confirmed that the UOWC had sufficient performance for practical, as presented in Section VI. 'Aerial' optical wireless communications based on the infrared data association (IrDA) standard have been demonstrated as practical already: optical wireless communication is useful in both air and water. Furthermore, communications over the sea surface directly were conducted in our test.

Considering the UOWC performance, Fig. 2 shows the prospective usage of the UOWC in the near future. If divers wear a diving computer linked with a UOWC modem, then the divers can access the internet through boats and aerial drones as network repeaters, where the boat works as a kind of mobile cells and drone works as a kind of mobile broad band modem. Underwater wireless LAN with optical communication (or Li-Fi: Light Fidelity) will be established in the system configuration.

Communication between underwater vehicles (V2V), such as manned observation vehicles and AUVs for example, enable sharing of information obtained through observations in water. Furthermore, swarm intelligence (SI) for AUVs will be developed greatly using the V2 V by UOWC.

However, long-distance communications for distances greater than 200 m are not easy for UOWC. Therefore, acoustic communications offers advantages for range. Consequently, acoustic communications are expected to be used over 200 m between vehicles and ships; optical communications are expected to be used under 200 m for vehicle-to-vehicle communications for sharing and retrieving information (see Fig. 3).

Fig. 3 Which communication mode to use corresponding to the range.

3. Optical Characteristics of the Sea in Various Conditions

3.1 Profiler for Underwater Optics

Water conditions affect light propagation. For that reason, measurement of attenuation at the communication area is important to use UOWC effectively.

A research group of SPAWAR categorized seawater into four types according to optical conditions [27]. These are good standards of optical conditions in the sea, but they do not include particle-related numerical information such as turbidity. The types are not practical information to develop or evaluate UOWC modems. However, measuring for each communication is not a practical method.

Therefore, we have strived to estimate optical characteristic of seawater from general seawater conditions measured using CTD, with which can measure turbidity and chlorophyll as well. If we were able to do this, the attenuation at an area where CTD had been deployed could be estimated without additional measurements. In other words, we could predict UOWC performance in the area.

To measure optical characteristics using CTD measurements, and to clarify their mutual relation, we have developed a profiler for underwater optics (see Fig. 4 and Table 1) [28]. The profiler can measure the respective intensities of 460 nm (blue), 525 nm (green), and 625 nm (red) light propagated through 0.9 m water. Furthermore, the scatter in water is also measured in nine colors of light having wavelengths are 370–635 nm. The profiler has a depth sensor, so the measurement are conducted with precise depth information. Because the profiler can work with an internal battery, we can operate it without shielded cables that have wires for power supply and communication. This is often called a CTD winch system (see Fig. 5).

3.2 Profiling Data Obtained Offshore of Okinawa and Yokokawa Dam

Measurements were taken with the profiler 33 times at 17 sea areas and at a dam lake from 2016 to 2018. Optical attenuations at respective wavelengths were quantified through measurements.

Some data of the measurements are presented in Fig. 6; panels (a–e) respectively present data measured at coastal waters near Kerama Islands in Okinawa, February 2018.

Fig. 4 Profiler for underwater optics.

Table 1 Specifications of the profiler.

Dimension	1.5 × 0.4 × 0.4 m
Weight in air	approx. 60 kg
Maximum operating depth	1,000 m
Measured items	Attenuation at 460, 525 and 625 [nm] Scatter at 370, 400, 435, 470, 505, 525, 550, 590 and 635 [nm] Conductivity, Temperature, Depth, Dissolve oxygen, Salinity, Chlorophyll, and Turbidity
Sensors for attenuation	Detector (PD): Hamamatsu Photonics 'c10439-09' Emitter (LED): Optosupply 'ostcxbcbc1e'
Sensors for scatter	JFE Advantech 'Multi-Exciter' (customized)
CTD	JEF Advantech 'Rinko Profiler'

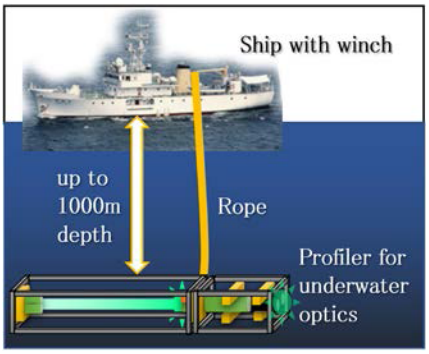

Fig. 5 Schematic diagram showing how to use the profiler.

The seawater at the area is very clear. The best communication channel for UOWC is expected there. Specifically, (a)(b)(c)(d) respectively stand for turbidity, chlorophyll, optical attenuation, and reflection. Turbidity is a relative index with the unit of formazin turbidity unit (FTU). When water has the same turbidity as that of a 1 ppm formazine solution, turbidity of the water is 1 FTU. Turbidity is measured using optical reflection by particles in infrared near 880 nm wavelength. Turbidity in the (a) was low, around 0.05 FTU up to 250 m depth; it fell to 0.01 FTU over 250 m depth.

Chlorophyll is measured by emitting blue light near 470 nm to the water and receiving fluorescence as green light from phytoplankton that absorb the blue light and which waste light energy as the green light. The chlorophyll in (b) was around 0.5 ppb (or μg/l) up to 250 m, but it fell to

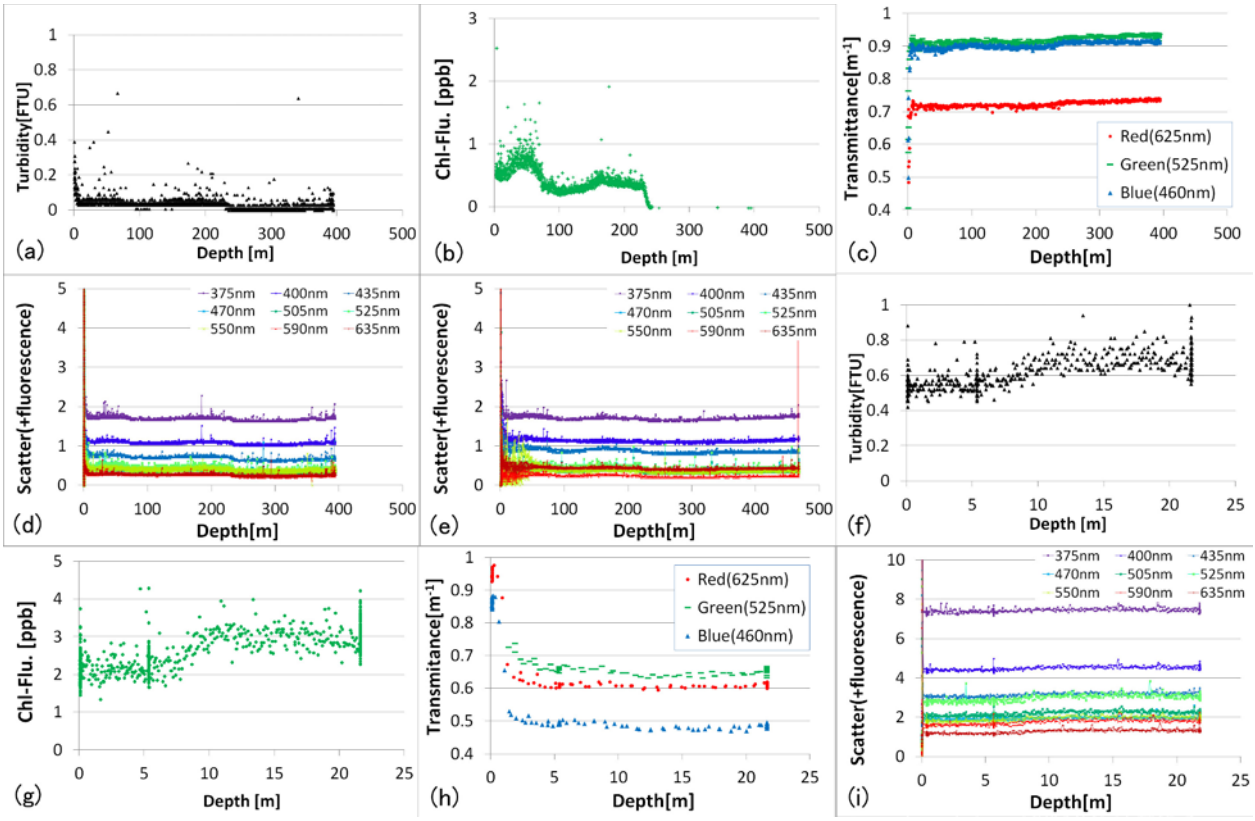

Fig. 6 Data measured by the profiler. (a)(b)(c)(d) are turbidity, chlorophyll, transmittance and reflectance respectively measured midnight at coastal waters near Kerama islands in Okinawa. (e) is measured at the same area of (d) daytime. (f), (g), (h) and (i) are turbidity, chlorophyll, transmittance and reflectance respectively are measured at Yokokawa dam lake in Fukushima prefecture.

less than 0.01 ppb, which is lower than the detection limit, at depths of less than 250 m. A jump of values is often measured where thermal layers exist.

Transmittance in (c) is a relative index of optical power passing through the medium, which is 1.0 in clear air. Transmittances were 0.90 at blue, 0.91 at green, and 0.72 at red up to 250 m depth. It went into 0.91 at blue, 0.93 at green, and 0.73 at red over 250 m depth. The transmittance of blue and green were high because the sea was clear. Green was slightly higher than blue at all depths. Red, which is a longer wavelength, had lower transmittance than the others. However, the value was near the upper limit, where the particles were sparse theoretically. Transmittances at 7 m were close to the transmittance at 250 m, so the transmittances were stable at all depths.

Scatter (+fluorescence) in (d) is optical power reflected by water with particles. However, fluorescence by some phytoplankton is included to a slight degree. The unit is just raw data. Data should be used to compare colors. All scatter (+fluorescence) was also stable at all depths. Light of 375 nm wavelength, which is violet, was reflected strongly, but 635 nm, which is red, was reflected weakly. Actually, 525 and 550 nm light was reflected slightly more than 470 nm and 505 nm.

Panel (e) shows reflection at the same area with (d) at noon: (d) was measured after sunset. Reflection at 550 nm was strong around 30 m depth. The change resulted from chlorophyll, which is active under sunlight.

Panels (f–i) respectively show measurements at the Yokokawa dam lake in Fukushima pref., Feb. 2018. Dam lakes have low circulation of water and often become dirty. Therefore, it is expected that the communication channel for UOWC is bad there.

Turbidity was around 0.6 FTU, chlorophyll was around 2.5 ppb. These were quite high, so transmittances were low at all colors. Transmittance of blue light was 0.49, green was 0.64, and red was around 0.61. The transmittance decrease was smaller in red. We confirmed using theoretical arguments that effects by suspended particles were small for red light. The reflection was strongest at 525 nm. Chlorophyll absorbs light at around 470 nm wavelength. One can infer that chlorophyll affects blue and green light strongly.

3.3 Optical Conditions in Japanese Seas

Figure 7 presents a relation between turbidity and transmittance. Figure 8 shows the relation between chlorophyll and transmittance. Those were calculated from our measurements conducted using the profiler. Exponential regressions with data at each wavelength are shown in each figure as

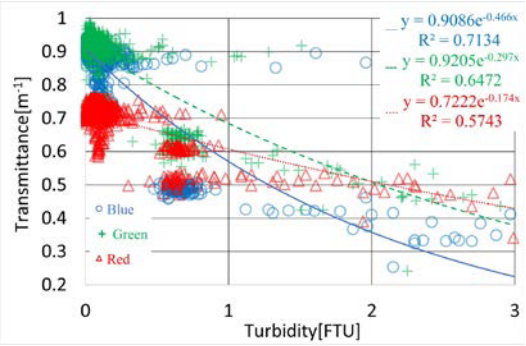

Fig. 7 Turbidity vs. transmittance.

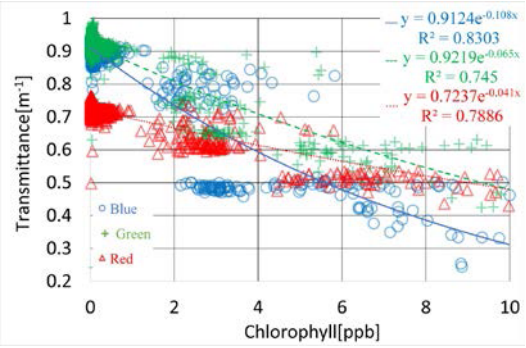

Fig. 8 Chlorophyll vs. transmittance.

expressions.

Transmittance values of blue, green, and red are respectively 0.91, 0.92, and 0.72 when both turbidity and chlorophyll are 0. Those values might be useful to consider its upper limits in sea surrounding Japan.

The coefficient of determination, R^2, is closer to 1 in Fig. 8 than in Fig. 7, which means that fitting of the regression expression in Fig. 8 is better than that shown in Fig. 7. It is better to refer to chlorophyll for estimating attenuation.

The regression expression of transmittance in red crosses the expression in blue and green. Actually, the transmittance of red becomes superior concomitantly with increasing turbidity or chlorophyll. The color red better than blue when turbidity is greater than 0.79 FTU. Red is better than green when turbidity is greater than 1.97 FTU. For chlorophyll, red is better than blue when it is greater than 3.46 ppb, and is better than green when it is greater than 10.09 ppb.

Figure 9 is created based on optical profiling. The figure shows turbidity, chlorophyll and transmittance at areas where the profiling has been done. The area is shown as a rectangular area with rounded corners; the values in the rectangle are measured results for the area. The background color represents the color of highest transmittance there. If the color is not uniform at all depths, the background is filled with the color gradation. If it is apparent that green is superior in transmittance from Fig. 9, then blue and red have

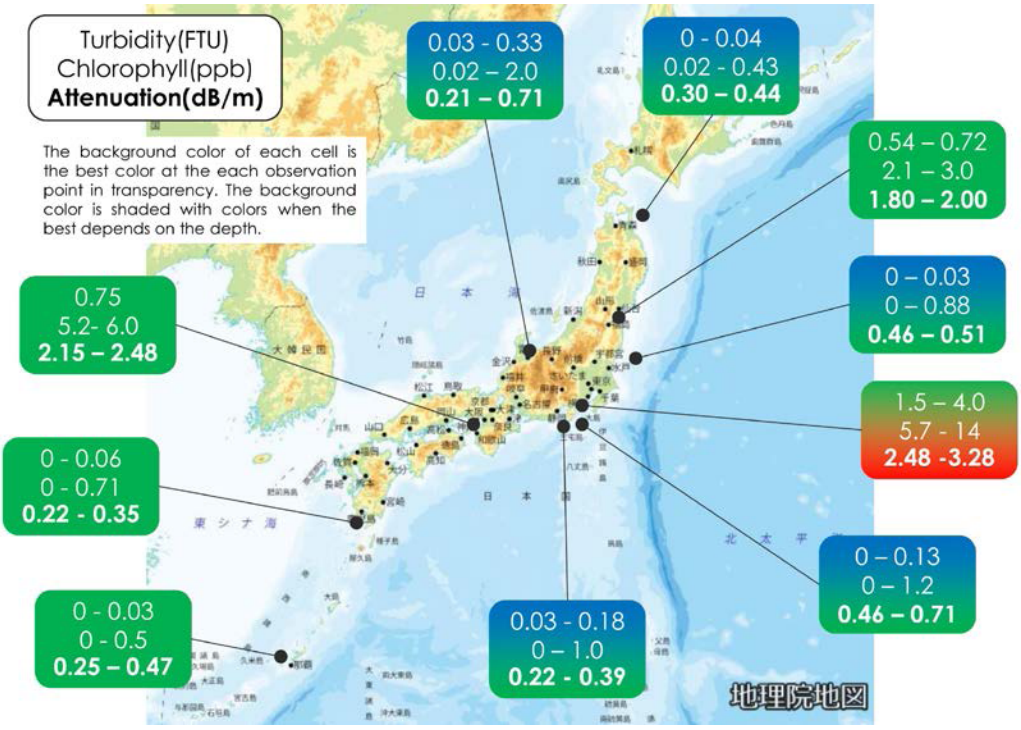

Fig. 9 Optical attenuation chart. Turbidity, chlorophyll and optical attenuation at the pointed area are shown. The background color of the rectangular with rounded corner means the color of highest transmittance there. If the color is not sole all the depth, the background is filled with the gradation of the colors. This figure uses a map from GSI.

good transmittance in some areas depending on the depth. Many reports have described that blue light has the best transmittance in clear water without particles. However, green light of 525 nm wavelength has better transmittance than blue light of 460 nm in many cases for the seas around Japan.

4. Communication Tests with a Prototype UOWC Modem

4.1 Prototype of UOWC Modem

The UOWC performance can be increased by changing the emission color. The most effective color depends on the water condition. That point was confirmed through our measurements conducted using the profiler for underwater optics. However, practical performance of UOWC is subject to external noise such as sunlight and flood lights of underwater vehicles, axis error of the light, and power consumption of the modem.

To estimate the practical performance in various sea conditions, a prototype UOWC modem were developed. Figure 10 shows the modem prototype. Figure 11 shows a block diagram of it. Table 2 presents specifications.

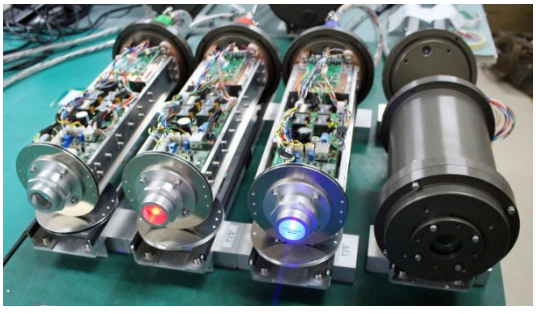

Fig. 10 LD units (from right to center) and PMT units (right) of the UOWC modem. Lights are adjusted in beam width through the lens in front of the light source. The dark gray cylinder is the pressure-proof housing with a glass window.

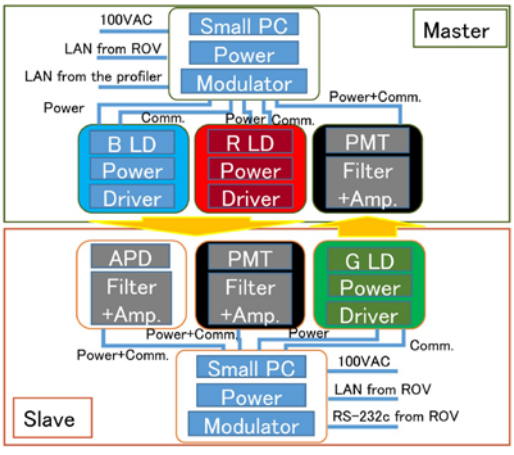

Fig. 11 Block diagram of the prototype modem.

The modem is composed of a main pressure vessel and three small pressure vessels. A small PC, a power supply and a modulator are in the main pressure vessel. Every small vessel has an LD, APD, and PMT with a sappier glass window. A pair of the modems is used in UOWC. One modem is the Master: it can communicate with the profiler for underwater optics and read the profile data to change the light color automatically depending on the data such as turbidity. Every small vessel can be connected to the main vessel, but a blue LD, red LD, and PMT are connected to the master side of the main pressure vessel.

The modem uses fiber-coupled LDs that emit high intensity laser light from the edge of optical fiber that gathers light from LDs. The modem can select a light emission color from blue (450 nm), green (525 nm), and red (640 nm). The beam focus can be adjusted through the lens in front of the multi-mode fiber.

The modem detector can be selected from PMT and an APD photodiode. The received optical power and the durability of these receivers were estimated via testing.

The communication speed is also selectable from 32 kbps to 20 Mbps depending on the error rate in the communications. A low-pass signal filter with a frequency is three times higher than the communication signal is usually used for communications testing.

An optical bandpass filter to suppress ambient light is set in front of the detector as needed. The half-power width of the filter is 25 nm.

The modulation is OOK, which is vulnerable to DC noise. Therefore, it is also important to compensate the change of the DC noise caused by drifting of the communication distance and ambient light. Auto gain control (AGC) is used in the modem to select an adequate threshold on the receiver circuits.

The light frequency is too high over 100 THz. In addition, the temperature dependence of the semiconductor light source is strong at all optical wavelengths because the energy bandgap, which is strongly related to the wavelength, changes according to temperature. These make a PLL loop on optics difficult in general electric circuits. Therefore, 4B/5B code that is used successfully for communications

Table 2 Specifications of the underwater optical wireless communication modem.

Weight	40 kg in air
Power consumption	350 W max.
Wavelength	450, 525, 640 nm
Max. output light power	>5 W
Beam angle	variable (depending on the lens)
Operating depth	up to 1000 m
Communication protocol	100 M Ethernet (TCP, UDP)
Modulation	OOK
Coding	4B/5B
APD	Bandwidth: 300–1070 nm Response: up to 48 MHz
PMT	Bandwidth: 230–920 nm Response: up to 24 MHz
Optical filter (in front of the detector)	Around 20 nm bandpass matched for each emitted color
LD	Optical power: over 5W

with optical fiber cable is adopted. Bit reversal occurs moderately for synchronization in the code. The bits on the code are changed from '1' to '0' or from '0' to '1' moderately for synchronizing the modems. Because the data are sent and received using TCP/IP protocol, underwater Wi-fi or Li-fi can be established easily with the modem.

4.2 Communication Test in a Pool and the Sea

On July 26, 2017, the modem was tested on the underwater vehicle *Kaiko*; its mother ship was the research vessel *Kairei*. The modems were installed to both the vehicle module and launcher module of *Kaiko*. The launcher module is like an underwater mobile base (see Fig. 12). The vehicle module moved away from the launcher module slowly while maintaining optical communication. The relative position of the vehicle and launcher were roughly confirmed using surveillance cameras on the launcher module (Fig. 13).

On the vehicle module, two transmitters and one detector were loaded. The transmitters had 3 and 20 deg beam width of blue LD. The detector was PMT and a green bandpass filter. We loaded one transmitter and two detectors on the launcher module. The transmitter had 20 deg beam width of green LD. The detectors were APD and PMT with a blue bandpass filter. Through the test, the beam width and optical power were changed and measured along with the communication speed. The range was increased step-by-step after measurements were taken at a given distance.

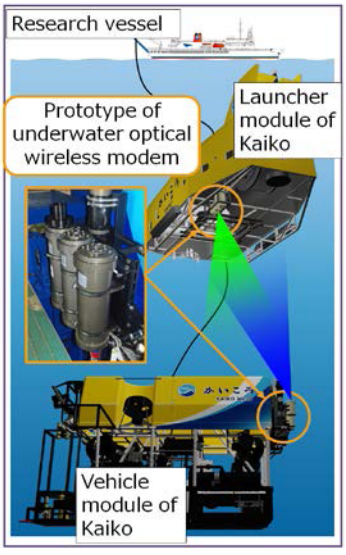

Fig. 12 Schematic diagram of the communication test in the sea.

Fig. 13 Top view from the launcher.

Through the test, APD and PMT had sufficient durability and no deterioration. Figure 14 presents the test results. The horizontal axis shows the communication range; the vertical axis shows the communication speed or clock rate of emitter and receiver. The power is an index that is roughly in proportion to the light projection power. We confirmed communication in the 120 m range at 20 Mbps in this test. It is approx. 100 times faster than acoustic communication conducted at the same distance.

Remote desktop connection from the vehicle to the launcher was achieved in 100 m range. Results proved that a stable LAN connection can be achieved between unstable underwater vehicles. Because the emitted colors of the light from each modem differed, light–light interference was suppressed efficiently in bi-directional communication.

The test area had abundant marine-snow (plankton carcasses), but the turbidity often became lower than 0.01 FTU. The marine-snows pose no great obstacle hindering UOWC. Furthermore, a floodlight of the launcher was turned on throughout the test. It proved the robustness of the modem against external disturbances.

On September 13, 2017, the modem was tested in a high-speed towing tank (see Fig. 15) owned by the Naval Systems Research Center of Acquisition, Technology and Logistics Agency. The length, the width, and the depth of the tank were, respectively, 350 m, 6 m, and 2.5 m. Inside the tank is a tunnel with a railway bogie over the tank. One modem was hung from the bogie into the tank. The other was set at the tank edge in the water.

The modem was tested without a rock in this setup. The beam widths were 3 and 0.3 deg in the test. The detectors were PMT. The test was conducted when the light in the tunnel turned on and off. The tank turbidity was less than 0.01 FTU, which is close to the turbidity in the sea test, whereas the chlorophyll was about 0.11 ppb.

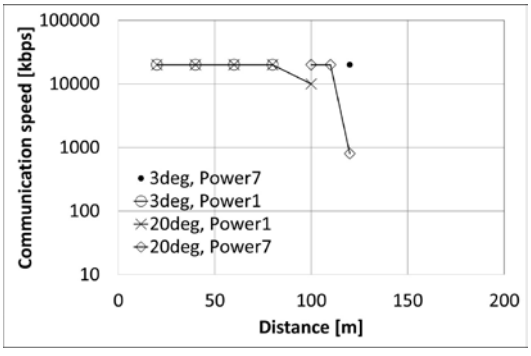

Fig. 14 Communication distance vs. speed at the test in the sea. Turbidity and chlorophyll were, respectively, approximately 0.01 FTU and 0.05.

Fig. 15 High-speed towing tank.

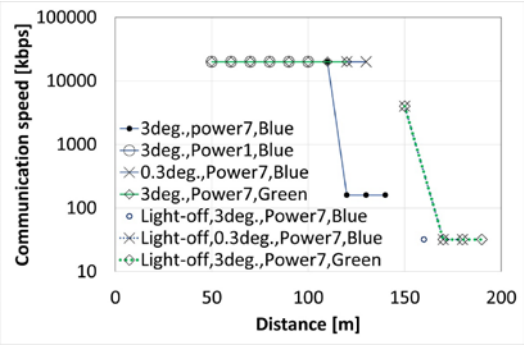

Fig. 16 Communication distance vs. speed at the test in the high speed towing tank. Turbidity and chlorophyll was approximately 0.01 FTU and 0.12, respectively.

Figure 16 presents test results. We confirmed communication at 190 m range when the light in the tunnel was turned off. The range was 140 m when the light was turned on. The UOWC is affected strongly by ambient light.

4.3 Estimation of the Communication Performance

The sea test confirmed 20 Mbps communication at 110 m range with 20 deg beam. Results are shown in Fig. 14. When the communication speed was changed to 800 kbps with the same beam width, the range was extended to 120 m. The range was extended because of the increase of optical power per data bit, i.e., increased S/N. When the power was 1–7, the optical emission intensity became 0.18 times; 10 Mbps communication speed at 100 m range was confirmed. Transmittance in the sea area was around 0.91/m. With range extended from 100 m to 110 m, the optical power become $(0.91)^{10} = 0.39$ times by transmission decay, $(100/110)^3 = 0.75$ times by diffusion decay. Furthermore, it became 0.5 times by changing speed from 20 Mbps to 10 Mbps. The total change was calculated theoretically as $0.39 \times 0.75 \times 0.5 = 0.15$ times. That value is close to 0.18, which was the change of emission power found from the sea test.

Results of the towing tank test, as shown in Fig. 16, closely approximated theoretical values. For example, the range was extended from 110 m to 140 m by decreasing the communication speed from 20 Mbps to 160 kbps using blue LD. The optical power is 0.059 times by transmission decay and 0.49 times by diffusion decay. The amount will result in 0.029 times. The optical power per bit became 125 times by the speed change. There must be margin of $125 \times 0.029 = 3.36$ times optical power S/N on the detector: communication at 500 kbps speed at the range became possible. The 160 kbps test was done immediately after 800 kbps in the tank test. Therefore, a gap separated the test results and theory.

The optical power per unit of illuminated area is increased by sharpening the beam. The communication performance is also expected to increase theoretically, but the performance did not improve drastically in our tests. For instance, 20 Mbps communication speed at 120 m range with 3 deg beam shows, as in Fig. 14, the results of sea testing: the communication was unstable. Furthermore, the communication range was extended from 110 m to 130 m by sharpening the beam from 3 deg to 0.3 deg, in Fig. 16, as results of towing tank testing.

The illumination area is $2\pi r^2(1 - \cos\theta)$, where the beam width is θ and the communication distance is r. When the beam width is sharpened from 3 deg to 0.3 deg, the light power per unit of area is expected to increase $(1-\cos(1.5\,\text{deg}))/(1-\cos(0.15\,\text{deg})) = 99.8$ times. Transmission decay is 0.092 times when the transmission distance changes from 110 m to 130 m, so S/N has a margin of $99.8 \times 0.092 = 9.18$ theoretically. However, the margin was apparently lost through axis error.

Results show that the stability of the platform, such as underwater robots, is important for UOWC. It is effective to use a gimbal mount and additional optical systems for axis error compensation.

Even more, the communication distance of 190 m with 3 deg beam of green LD when the speed was 32 kbps was achieved in the towing tank test. The actual green LD optical power was 4.93 W. The maximum receiver detection sensitivity was 0.025 pW/mm^2 (@10 Mbps) for this circuit configuration. The theoretical communication distance was estimated as 220 m.

The relations between communication speed and attenuation for respective beam widths and sea conditions are shown in Fig. 17. The relations are generated from the results above and their interpolation. The communication speed of all graphs in the figure is 10 Mbps. The blue line shows results based on sea tests. The red line is based on the actual optical power and the maximum detection sensitivity.

At 2.3 FTU, close to the value at the surface of the Seto Inland Sea, the communication range is up to 10 m with a 90 deg beam and around 20 m with a 3 deg beam. Figure 18 presents an enlarged view of Fig. 17 around the 100 m range. At the area where turbidity is lower than 0.1 FTU, as at coastal areas near Okinawa, the communication range is greater than 60 m with a 90 deg beam and greater than 150 m with a 3 deg beam.

Table 3 presents relations between communication speed and range for each beam where the turbidity is assumed as 0.01 FTU, chlorophyll is 0.01 ppb., and light color

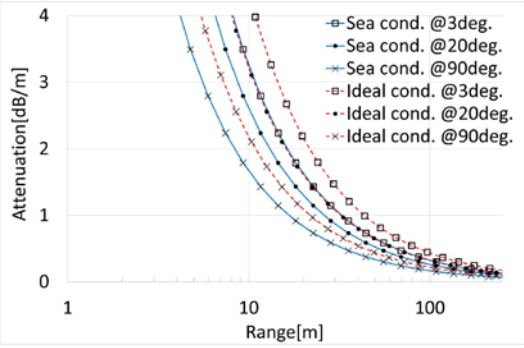

Fig. 17 Range vs attenuation at 10 Mbps.

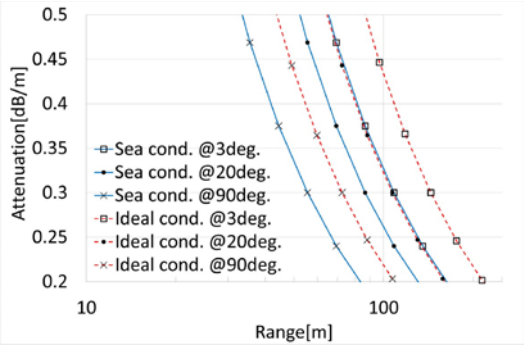

Fig. 18 Enlarged view of Fig. 16 around 100 m range.

Table 3 Expected Ethernet communication speed. Turbidity is assumed as around 0.01 FTU. Chlorophyll is 0.01 ppb. The light is blue (460 nm).

Range [m]	Speed [bps] @3 deg beam	@20 deg beam	@90 deg beam
20	Over 10 G	10 G	1 G
50	5 G	1 G	100 M
100	100 M	10 M	1 M
150	1 M	Low	NG

is blue (460 nm). The speed in the table is shown as the Ethernet standard speed. 1 Mbps speed at 150 m range and 100 Mbps speed at 100 m range width 3 deg beam represent reasonable performance. In addition, 1 Mbps speed at 100 m and 1 Gbps speed at 20 m with a 90 deg beam are reasonable.

4.4 Communication Test Between Air and Underwater

We conducted extra sea tests with modems set in air and water for mutual direct communication through the sea surface. The modems were set on the edge of a tower, which was then sunk to midway, where one modem was in air and the other was in water (Fig. 19). The sea surface was constantly disturbed by waves (Fig. 20). The optical characteristics in air are slightly different in water because the modems were designed for underwater use. However, the change is negligible. The wave height is around 1 m through the test day. Therefore, the beam passage through the sea surface was disturbed by reflection, absorption, refraction, and diffusion at the sea surface. In spite of those disturbance factors, communication at 20 Mbps through 5 m of air and 5 m of the

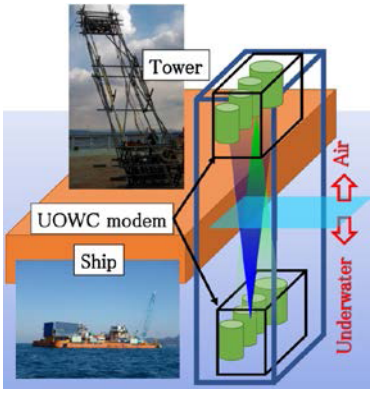

Fig. 19 Schematic diagram showing communication testing between air and under water.

Fig. 20 Lookdown image from air to underwater side modem.

underwater channel was achieved.

5. Conclusion

Recent trends of UOWC-related study specifically examine channel characterization, modulation, and coding techniques. Those studies have demonstrated that UOWC is expected to offer high speed Ethernet links as Li-Fi, and be useful for divers and underwater drones for mutual communication up to 200 m range.

We developed a profiler for underwater optics and quantified optical attenuations and reflections at each wavelength 33 times for 17 sea areas and at a dam lake during 2016–2018. Relations between turbidity, chlorophyll, and transmittance were demonstrated from profiler measurements. An optical attenuation chart was demonstrated.

The prototype UOWC modem was developed with an emitter and receivers as LD and APD or PMT, respectively. Sea tests for the modem were conducted and established UOWC at 20 Mbps at a 120 m range. A pool test demonstrated that UOWC was possible at 32 kbps at a 190 m range established. The performance of the prototype modem was analyzed based on these results, and predicted several beam widths without external noise or platform motion.

We confirmed that UOWC is sufficient to establish high-speed communications as Li-Fi. A UOWC modem with omnidirectional directivity and a compensator for optical

axis error are being developed now. These modems are expected to clear the way for underwater IoT in the near future.

Acknowledgments

This work was supported by the Innovative Science And Technology Initiative for Security, ATLA, Japan.

References

[1] B. Wozniak and J. Dera, Atmospheric and Oceanographic Sciences Library (Book 33), Springer, 2011.
[2] Ultrasonic handbook Editorial Board, Ultrasonic handbook, Maruzen, 1999.
[3] N.G. Jerlov, Optical Oceanography, Elsevier, 1969.
[4] S. Nakao, Research of underwater transmission of laser, thesis of Keio Univ., 1979 (in Japanese).
[5] C. Gabriel, M.A. Khalighi, S. Bourennane, P. Leon, and V. Rigaud, "Channel modeling for underwater optical communication," 2011 IEEE GLOBECOM Workshops (GC Wkshps), pp.833–837, Houston, TX, 2011.
[6] R.C. Smith and K.S. Baker, "Optical properties of the clearest natural waters (200–800 nm)," Appl. Opt., vol.20, no.2, pp.177–184, 1981.
[7] W. Breves and R. Reuter, "Bio-optical properties of gelbstoff in the Arabian Sea at the onset of the southwest monsoon," J. Earth Syst. Sci., vol.109, no.4, pp.415–425, Dec. 2000.
[8] D.A. Hansell and C.A. Carlson, Biogeochemistry of Marine Dissolved Organic Matter, Academic Press, Amsterdam, The Netherlands, 2014.
[9] V.I. Haltrin, "Chlorophyll-based model of seawater optical properties," Appl. Opt., vol.38, no.33, pp.6826–6832, 1999.
[10] C.D. Mobley, B. Gentili, H.R. Gordon, Z. Jin, G.W. Kattawar, A. Morel, P. Reinersman, K. Stamnes, and R.H. Stavn, "Comparison of numerical models for computing underwater light fields," Appl. Opt., vol.32, no.36, pp.7484–7504, 1993.
[11] S. Arnon, J. Barry, G. Karagiannidis, R. Schober, and M. Uysal, Advanced Optical Wireless Communication Systems, Cambridge Univ. Press, Cambridge, U.K., 2012.
[12] J. Li, Y. Ma, Q. Zhou, B. Zhou, and H. Wang, "Monte Carlo study of pulse response of underwater optical channel," Opt. Eng., vol.51, no.6, Art. no.066001, June 2012.
[13] A. Choudhary, V. Jagadeesh, and P. Muthuchidambaranathan, "Pathloss analysis of NLOS underwater wireless optical communication channel," Proc. Int. Conf. Electron. Commun. Syst. (ICECS), pp.1–4, Coimbatore, India, Feb. 2014.
[14] F. Hanson and M. Lasher, "Effects of underwater turbulence on laser beam propagation and coupling into single-mode optical fiber," Appl. Opt., vol.49, no.16, pp.3224–3230, May 2010.
[15] M. Khalighi and M. Uysal, "Survey on free space optical communication: A communication theory perspective," IEEE Commun. Surveys Tuts., vol.16, no.4, pp.2231–2258, Fourth Quart., 2014.
[16] I. Lu and Y. Liu, "205 Mb/s LED-based underwater optical communication employing OFDM modulation," Proc. OTO2018, Kobe, Japan, 2018.
[17] W.C. Cox, J.A. Simpson, C.P. Domizioli, J.F. Muth, and B.L. Hughes, "An underwater optical communication system implementing Reed–Solomon channel coding," Proc. IEEE/MTS OCEANS, pp.1–6, Quebec City, QC, Canada, 2008.
[18] M. Saotome, Y. Kozawa, Y. Umeda, and H. Habuchi, "Differential-OOK system for underwater visible light communications," Proc. NCSP'16, Hawaii, USA, 2016.
[19] J. Everett, "Forward-error correction coding for underwater free-space optical communication," M.S. thesis, Dept. Elect. Eng., North Carolina State Univ., Raleigh, NC, USA, 2009.
[20] C. Pontbriand, N. Farr, J. Ware, J. Preisig, and H. Popenoe, "Diffuse high-bandwidth optical communications," Proc. IEEE/MTS OCEANS, pp.1–4, Quebec City, QC, Canada, 2008.
[21] N. Farr, J. Ware, C. Pontbriand, T. Hammar, and M. Tivey, "Optical communication system expands CORK seafloor observatory's bandwidth," OCEANS 2010 MTS/IEEE SEATTLE, pp.1–6, Seattle, WA, 2010. doi: 10.1109/OCEANS.2010.5663951
[22] M. Doniec, A. Xu, and D. Rus, "Robust real-time underwater digital video streaming using optical communication," Proc. IEEE Int. Conf. Robot. Autom. (ICRA), pp.5117–5124, Karlsruhe, Germany, 2013.
[23] H.M. Oubei, J.R. Duran, B. Janjua, H.-Y. Wang, C.-T. Tsai, Y.-C. Chi, T.K. Ng, H.-C. Kuo, J.-H. He, M.-S. Alouini, G.-R. Lin, and B.S. Ooi, "4.8 Gbit/s 16-QAM-OFDM transmission based on compact 450-nm laser for underwater wireless optical communication," Opt. Express, vol.23, no.18, pp.23302–23309, 2015.
[24] W.C. Cox, K.F. Gray, J.A. Simpson, B. Cochenour, B.L. Hughes, and J.F. Muth, "A MEMS blue/green retroreflecting modulator for underwater optical communications," Proc. IEEE/MTS OCEANS, pp.1–4, Seattle, WA, USA, 2010.
[25] https://www.yuden.co.jp/cms/wp-content/uploads/sites/2/2014/05/11e2ae1acb53cc88d38fe788bc9a1f4b.pdf
[26] https://www.khi.co.jp/news/detail/20171121_1.html
[27] F. Hanson and S. Radic, "High bandwidth underwater optical communication," Appl. Opt., vol.47, no.2, pp.277–283, 2008.
[28] T. Sawa, N. Nishimura, T. Kumagai, A. Ichikawa, and S. Goto, "A profiler for underwater optics," 2016 Techno-Ocean, no.1D-3, pp.189–194, Kobe, 2016.

Takao Sawa received B.S. and M.S. degrees in mechatronics from Nagoya University, Japan in 1998 and a Ph.D. in electro-communications from the University of Electro-communications, Japan in 2007. Currently, he is an Engineering Researcher at the Department of Marine Technology Center, Japan Agency for Marine–Earth Science and Technology, Japan.

Naoki Nishimura was born in Yamaguchi, Japan in 1968. He received a B.E. degree in Computer Science from Okayama University in 1991. Since then, he has been with the Magnetometer Equipment Department.

Koji Tojo received B.E. and M.E. degrees in Mechanical Engineering from Osaka University in 1989 and 1991, respectively. During 1991–2004, he was with the Technology Research Laboratory, Shimadzu Corp., Kyoto, Japan. Since 2004, he has been with Device Department, Shimadzu Corp., Atsugi Japan. His current research interests include the development of compact solid state lasers for industrial applications.

Shin Ito was graduate information processing course of Nihondenshi Pro-industry Technical School in 1987, and started working in sAs Corp. He developed PBX and firmware for telephones and information devices.